Hyperfine Interact (2016) 237: 141
DOI 10.1007/s10751-016-1355-9

New superconductivity dome in $LaFeAsO_{1-x}F_x$ far away from magnetism and accompanied by structural transition

J. Yang[1] · Guo-qing Zheng[1,2]

Published online: 5 October 2016

Abstract We report on the discovery and novel physics of a new superconductivity dome in $LaFeAsO_{1-x}F_x$ with high-doping rate ($0.25 \leq x \leq 0.75$) synthesized by using the high-pressure technique. The maximal critical temperature $T_c = 30$ K peaked at $x_{opt} = 0.5 \sim 0.55$, which is even higher than that at $x \leq 0.2$. By nuclear magnetic resonance (NMR), we find that the new superconducting dome is far away from a magnetically ordered phase without low-energy magnetic fluctuations. Instead, NMR and transmission electron microscopy measurements indicate that a $C4$ rotation symmetry-breaking structural transition takes place for $x > 0.5$ above T_c. The electrical resistivity shows a temperature-linear behavior around the doping level where the crystal transition temperature extrapolate to zero and T_c is the maximal, suggesting the importance of quantum fluctuations associated with the structural transition. Our results point to a new paradigm of high temperature superconductivity.

Keywords Iron-based superconductors · New superconductivity dome · NMR · TEM · Structural phase transition

1 Introduction

Iron pnictides are a new class of high temperature superconductors, which was discovered in early 2008 [1]. To date, the highest transition temperature (T_c) in bulk iron-based

This article is part of the Topical Collection on *Proceedings of the International Conference on Hyperfine Interactions and their Applications (HYPERFINE 2016), Leuven, Belgium, 3-8 July 2016*

✉ J. Yang
yangjie@iphy.ac.cn

[1] Institute of Physics and Beijing National Laboratory for Condensed Matter Physics, Chinese Academy of Sciences, Beijing 100190, PR China

[2] Department of Physics, Okayama University, Okayama 7008530, Japan

superconductors has been raised up to 55 K [2]. Like the cuprates and heavy-fermion compounds, superconductivity in iron pnictides emerges in the vicinity of antiferromagnetism, which leads to proposals that superconductivity in these materials is mediated by spin fluctuations associated with the close-by magnetically-ordered phase [3, 4]. The prototype iron-pnictide LaFeAsO is an ordered antiferromagnet and becomes superconducting when substituting fluorine (F) for a part of oxygen (O). The superconducting region has a dome-like shape against the F-content x, while x could not exceed 0.2 [1, 5, 6]. The highest T_c = 27 K is found at $x = 0.06$ where exists strong low-energy spin fluctuations as evidenced by nuclear magnetic resonance (NMR) [6].

In this work, we have succeeded in synthesizing a series of high-doping samples of $LaFeAsO_{1-x}F_x$ with $0.25 \leq x \leq 0.75$ by high-pressure synthesis technique [7]. The T_c forms a new dome shape peaked at $x_{opt} = 0.5 \sim 0.55$ with a maximal $T_c = 30$ K below which diamagnetism appears (the electrical resistivity starts to drop at $T_c^{\rho} \sim 40$ K). The spin-lattice relaxation rate $(1/T_1)$ divided by temperature (T), $1/T_1T$ revealed that the new dome is far away from a magnetically ordered phase and there is no sign of low-energy magnetic fluctuations. Instead, above the dome and for $x > 0.5$, we find a new type of phase transition below which a four-fold symmetry ($C4$ rotation symmetry) is broken. The electrical resistivity shows a T-linear dependence around x_{opt}, where the structural transition temperature extrapolates to zero. These results suggest that there may be a new route to high temperature superconductivity.

2 Experimental

The polycrystalline samples of $LaFeAsO_{1-x}F_x$ (with nominal fluorine content $x = 0.25$, 0.3, 0.4, 0.5, 0.55, 0.6, 0.65, 0.7 and 0.75) were prepared by the high pressure synthesis method [2]. The starting materials LaAs, Fe, Fe_2O_3 and FeF_2 were mixed together according to the nominal ratio, then grounded into fine powder and pressed into pellets. The pellets were sealed in boron nitride crucibles and sintered in a six-anvil high-pressure synthesis apparatus under a pressure of 6 GPa at 1250°C for 2-4 hours.

The lattice parameters of the samples were determined by powder X-ray diffraction (XRD) with Cu Kα radiation. The T_c was determined by both DC susceptibility using a superconducting quantum interference device (Quantum Design) and AC susceptibility using an $insitu$ NMR coil. For NMR measurements, The NMR spectra were obtained by scanning the RF frequency and integrating the spin echo at a fixed magnetic field H_0. The spin-lattice relaxation time T_1 was determined by using the saturation-recovery method, and the nuclear magnetization was fitted to $1 - M(t)/M(\infty) = 0.1exp(-t/T_1) + 0.9exp(-6t/T_1)$ expected for the $I = 3/2$ central transition peak, where $M(t)$ is the nuclear magnetization at time t after the single saturation pulse [8]. The transmission electron microscope (TEM) experiments were done on a JEOL 2100F TEM.

3 Results and discussion

Figure 1 shows the lattice parameters of $LaFeAsO_{1-x}F_x$ obtained by powder XRD. The main phase of all samples adopts the same tetragonal ZrCuSiAs structure. The tetragonal a-axis length decreases progressively with increasing F-content x. This result implies that the doping does increase with increasing x. Although our NMR and TEM measurements

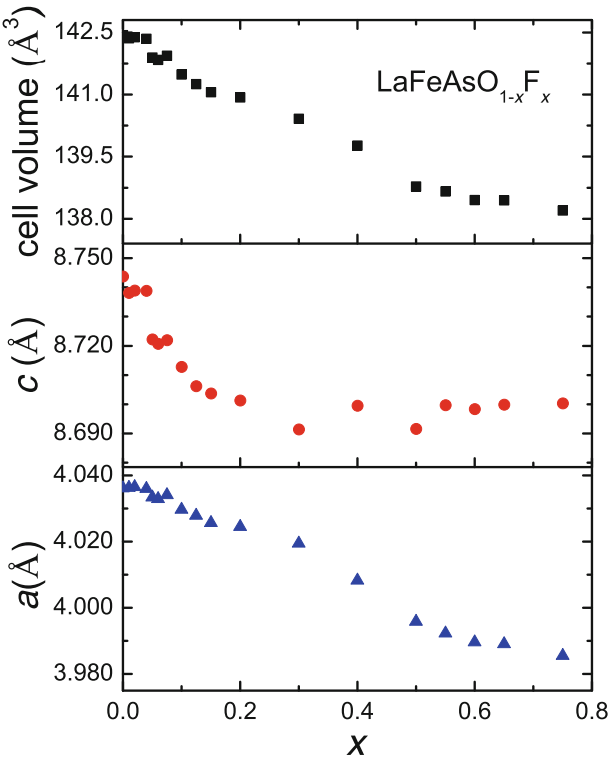

Fig. 1 The room temperature lattice parameters of $LaFeAsO_{1-x}F_x$ obtained by powder XRD. For $x = 0 \sim 0.2$, the data are taken from Ref. [5]

revealed that $LaFeAsO_{1-x}F_x$ ($x \geq 0.6$) has orthorhombic *Cmma* symmetry at room temperature (see below for more details), our Lab XRD are unable to distinguish the subtle change between orthorhombic a and b axes. We therefore adopted the tetragonal notation for all x to analyze the lattice parameters.

Figure 2a shows the DC susceptibility for $LaFeAsO_{1-x}F_x$ ($0.25 \leq x \leq 0.75$).The onset temperature of the diamagnetism is defined as T_c, which reaches the highest value of 30 K at $x = 0.55$. The large superconducting volume fractions of these samples as shown in Fig. 2a, together with the clear decrease of ^{75}As spin-lattice relaxation rate $1/T_1$ below T_c (see Fig. 9), ensure the bulk nature of the superconductivity. Figure 2b and c show the temperature dependence of the electrical resistivity ρ. We fit the resistivity data by the equation $\rho = \rho_0 + AT^n$. In Landau-Fermi liquid theory, the exponent $n = 2$ is expected for a conventional metal. However, $n < 2$ are obtained for all x, which suggest a non-Fermi liquid behavior. Most remarkably, for x=0.5 a T-linear behavior ($n = 1$) is observed over the range of 60 K$< T <$ 110 K, and for $x = 0.55$ over the range of 33 K $< T <$ 140 K.

Figure 3 shows the phase diagram that depicts the new superconductivity dome and the symmetry-breaking structural phase transition boundary. The evolution of the exponent n with the Fluorine content x is also shown in Fig. 3b. Note that neither F-doping nor oxygen-deficiency was able to go beyond $x = 0.2$ in the past, and the new superconducting dome in the high-doping region is unprecedented.

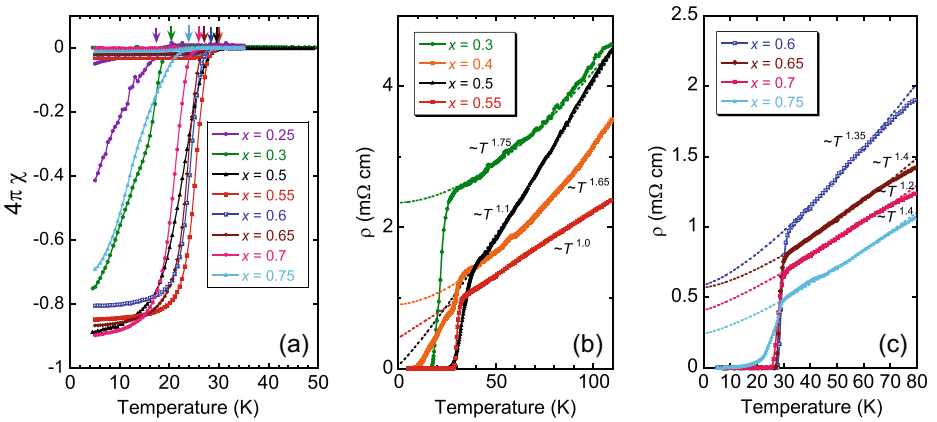

Fig. 2 The DC susceptibility and electrical resistivity of $LaFeAsO_{1-x}F_x$. **a** The DC susceptibility data measured with an applied magnetic field of 10 Oe. The arrows indicate the on-set temperature of the diamagnetism for each sample, which is defined as T_c. **b**, **c** The low temperature electrical resistivity. The dashed lines are the fittings to $\rho(T) = \rho_0 + AT^n$ by a sliding power law fitting over the temperature range shown

Below we elaborate how the structural phase transition with a four-fold ($C4$) symmetry breaking is probed by ^{75}As NMR. The asymmetry parameter η which describes the in-plane anisotropy is defined as,

$$\eta = \frac{\nu_x - \nu_y}{\nu_x + \nu_y} \tag{1}$$

where $\nu_\alpha = \frac{eQ}{4I(2I-1)} V_{\alpha\alpha}$ ($\alpha = x, y, z$) is the nuclear quadrupole resonance (NQR) frequency, $V_{\alpha\alpha} = \frac{\partial^2 V}{\partial \alpha^2}$ is the electric field gradient (EFG) tensor and V is the electrical potential. If a $C4$ symmetry exists in the ab-plane, $V_{xx} = V_{yy}$ so that $\eta = 0$. When the $C4$ symmetry is broken, η becomes finite.

Figure 4a shows the ^{75}As NMR spectra of the magnetically-aligned grains obtained by taking the advantage that the magnetic susceptibility is larger in the ab-plane than that along the c-axis [9]. For the $I = 3/2$ central transition line, when a magnetic field is applied along the principal axis z, the observed resonance frequency to the second order can be written as [10],

$$\nu_{res} = (1 + K)\nu_L + \frac{(\nu_x - \nu_y)^2}{12(1 + K)\nu_L} \tag{2}$$

where $\nu_L = \gamma_N H_0$ is the Larmor frequency, γ_N is the nuclear gyromagnetic ratio and K is the Knight shift. The second term is due to the nuclear quadrupole interaction. In undoped LaFeAsO at high temperature, the EFG principal axes x, y, z coincide with the crystal a, b, c axes [11].

For our magnetically-aligned powder sample with $H_0 \parallel ab$-plane, the second term of (2) is expressed as

$$\frac{3\nu_c^2}{16(1 + K)\nu_L}(1 + \frac{\eta^2}{9}) \tag{3}$$

According to (2) and (3), the plot of $\Delta\nu/\nu_L = (\nu_{res} - \nu_L)/\nu_L$ against ν_L^{-2} under different field H_0 will give K and $\nu_c^2(1 + \frac{\eta^2}{9})$, through the intersection of the vertical axis and the

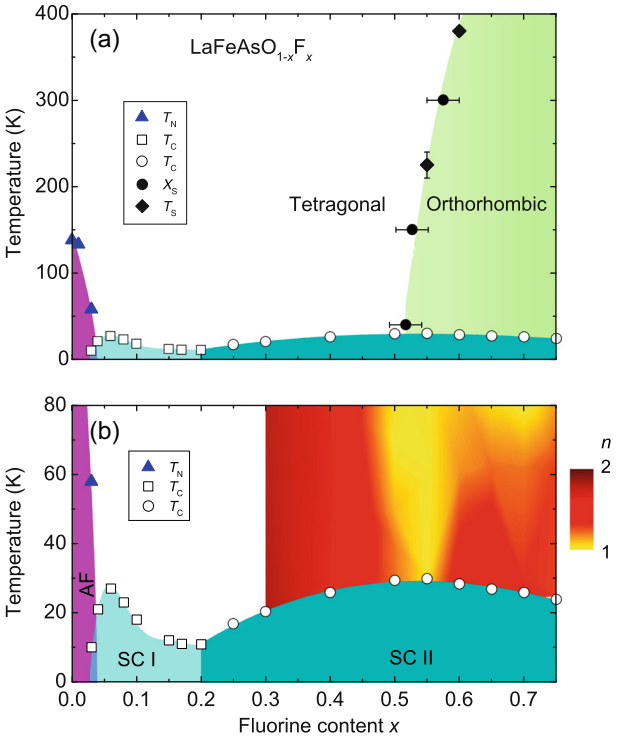

Fig. 3 The obtained phase diagram of $LaFeAsO_{1-x}F_x$. AF, SC I and SC II denotes the antiferromagnetically ordered phase, the superconducting phase obtained by conventional solid-state method and by high-pressure synthesis, respectively. **a** Doping dependence of the magnetic (T_N), superconducting (T_c) and structural transition temperatures (T_s). The T_N and T_c in SC I are taken from ref. [6]. The T_s for $x = 0.55$ and 0.6 was obtained from NMR and TEM measurements, respectively. x_s is the critical F-concentration at which the structure transition takes place. **b** The evolution of the exponent n obtained by fitting the electrical resistivity to a relation $\rho(T) = \rho_0 + AT^n$

slope, respectively. When a $C4$ symmetry breaking takes place so that η changes from zero to nonzero, the value of $\nu_c^2(1+\frac{\eta^2}{9})$ varies around the transition temperature. Figure 4b shows an example of such plot for the compound $LaFeAsO_{0.45}F_{0.55}$.

Through the same procedure, we obtained the evolution of $\nu_c\sqrt{1+\frac{\eta^2}{9}}$ as a function of x and temperature as shown in Fig. 5a and b. It can be seen that $\nu_c\sqrt{1+\frac{\eta^2}{9}}$ changes progressively as x increases. This result indicates further that the doping does increase with increasing x, since ν_c changes linearly with the real doping level [6]. At three representative temperatures, the x dependence of $\nu_c\sqrt{1+\frac{\eta^2}{9}}$ shows a crossover at a certain x_s. For the temperature variation, this quantity is temperature independent except for $x = 0.55$. There is a clear transition taking place between 250 and 200 K for $x = 0.55$, and the middle point of the transitions is defined as T_s. The above results indicate that η undergoes an abrupt increase when crossing x_s or T_s, and we plotted the obtained x_s and T_s in Fig. 3a. It is worthwhile pointing out that the phase transiton line extrapolates to zero at $x \sim 0.5$, where the electrical resistivity shows a T-linear behavior.

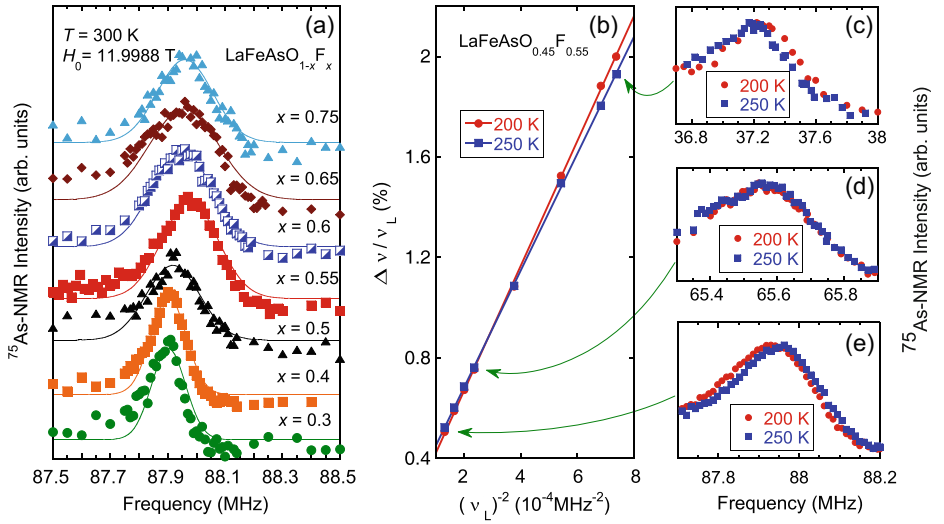

Fig. 4 **a** Magnetically aligned ^{75}As NMR central transition (the m = -1/2 ↔ 1/2 transition) spectra with $H_0 \parallel ab$-plane. **b** The procedure to obtain the quantity $\nu_c^2(1 + \frac{\eta^2}{9})$. The K and $\nu_c^2(1 + \frac{\eta^2}{9})$ are obtained through the intersection with the vertical axis and the slope of the $\Delta\nu/\nu_L$ versus ν_L^{-2} line, respectively. **c**-**e** The corresponding NMR spectra for three representative fields H_0 = 4.9983 T, 8.9232 T and 11.9988 T at T = 200 K and 250 K

The abrupt change of η crossing x_s is further confirmed by ^{139}La NQR measurements. Theoretically the three NQR transition lines for the I = 7/2 La nuclei are equally separated when $\eta = 0$, but unequally shifted for nozero η. This is the truth for our ^{139}La NQR spectra as shown in Fig. 5c. Our results reveal that $\eta = 0$ for x = 0.3, but η = 0.21 for x = 0.55. Thus, above the new dome, we find a structural phase transition from a four fold symmetry at high temperature to a lower symmetry at low temperature by ^{75}As NMR and ^{139}La NQR.

Furthermore, we have directly confirmed the structural transition by TEM. Figure 6a–c shows the [001] zone-axis electron diffraction patterns for x = 0.55 during a heat cycling

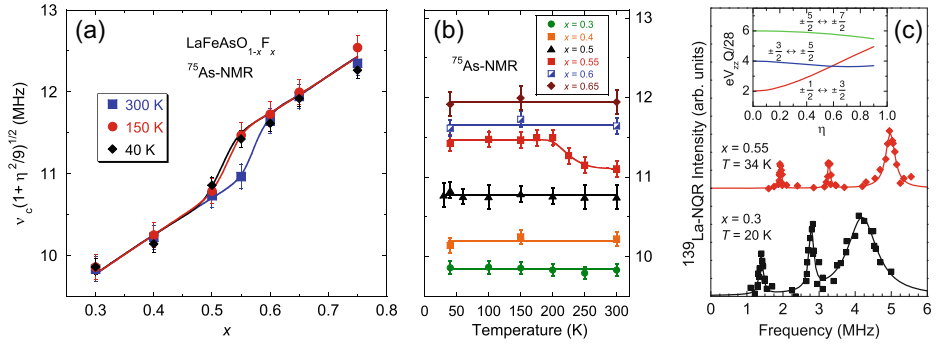

Fig. 5 The structural phase transition evidenced by asymmetry parameter η. **a** $\nu_c\sqrt{1+\eta^2/9}$ plotted against F-content x at T=300, 150 and 40 K. **b** $\nu_c\sqrt{1+\eta^2/9}$ as a function of temperature. The solid curves indicate the variation trend of the quantities. **c** ^{139}La-NQR spectra for x = 0.3 and 0.55. The inset shows the evolution of the three transition frequencies with increasing η

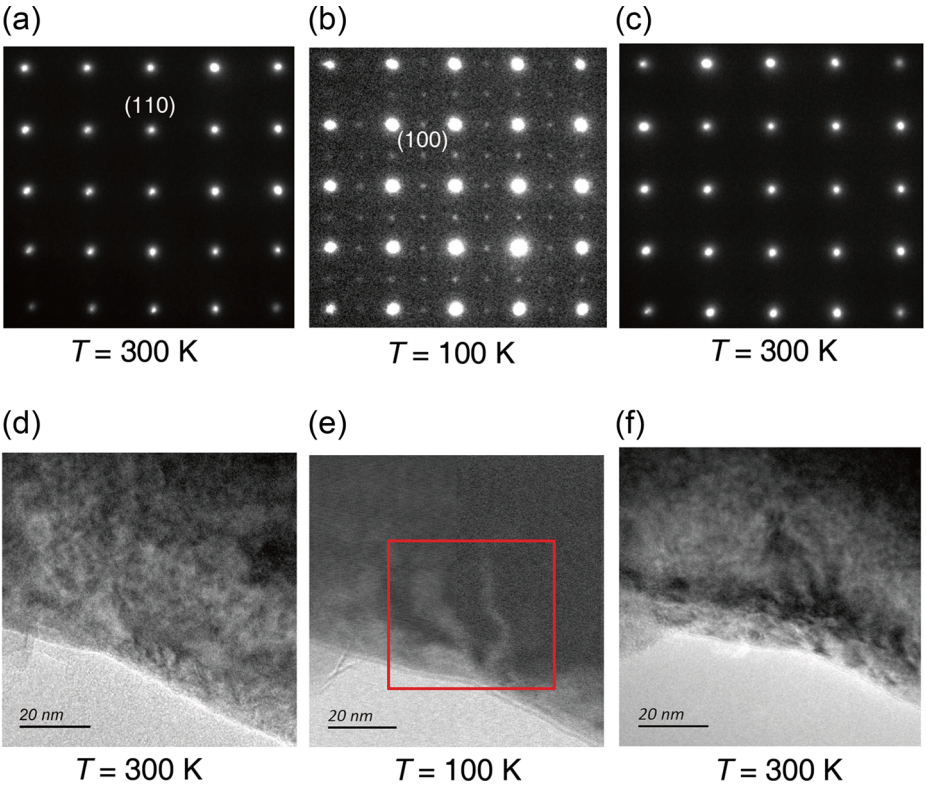

Fig. 6 Electron diffraction patterns of $LaFeAsO_{0.45}F_{0.55}$ during a heat cycling of 300 K (**a**) → 100 K (**b**) → 300 K (**c**). (**d**-**f**) show the microstructures during the cycling. Domain structure appeared at T=100 K is marked by the red rectangle

of 300 K → 100 K → 300 K, and (d-f) the corresponding microstructures. At T = 300 K, the crystal structure is tetragonal with $C4$ symmetry. At T = 100 K, however, additional spots appear at (100) positions, which unambiguously indicates that the $C4$ symmetry is lowered at low temperature. Domain structures also appear at T = 100 K as shown in Fig. 6e, which are due to twinning domains energetically preferred by structural relaxation following the phase transition. After cooling to 100 K and carrying out the TEM experiments there, the sample was heated back to 300 K, then the tetragonal symmetry was recovered and the domain sturctures were absent. Remarkably, the observed TEM features in $LaFeAsO_{0.45}F_{0.55}$ resemble the results in parent compounds LaFeAsO and NdFeAsO, where a tetragonal-to-orthorhombic structural transition takes place at T_s = 135 K [12].

We conducted TEM measurements on samples of other doping levels and also obtained evidence for the structural transition. Figure 7 shows the TEM results for x = 0.6. At T = 300 K, the (100) spots and domain structures indicate that $C4$ symmetry has already been broken. Upon heating from room temperature, the (100) spots disappeared at T = 380 K. We therefore identified the structural transition temperature T_s = 380±5 K for x = 0.6 and plotted it in Fig. 3a. Figure 7d and e show the additional TEM results at T = 300 K for x = 0.6. A splitting of the (640) diffraction spot is visible after rotating the image by 4 degrees, which also assures that $C4$ symmetry is broken. Figure 7 (f) shows the TEM image taken

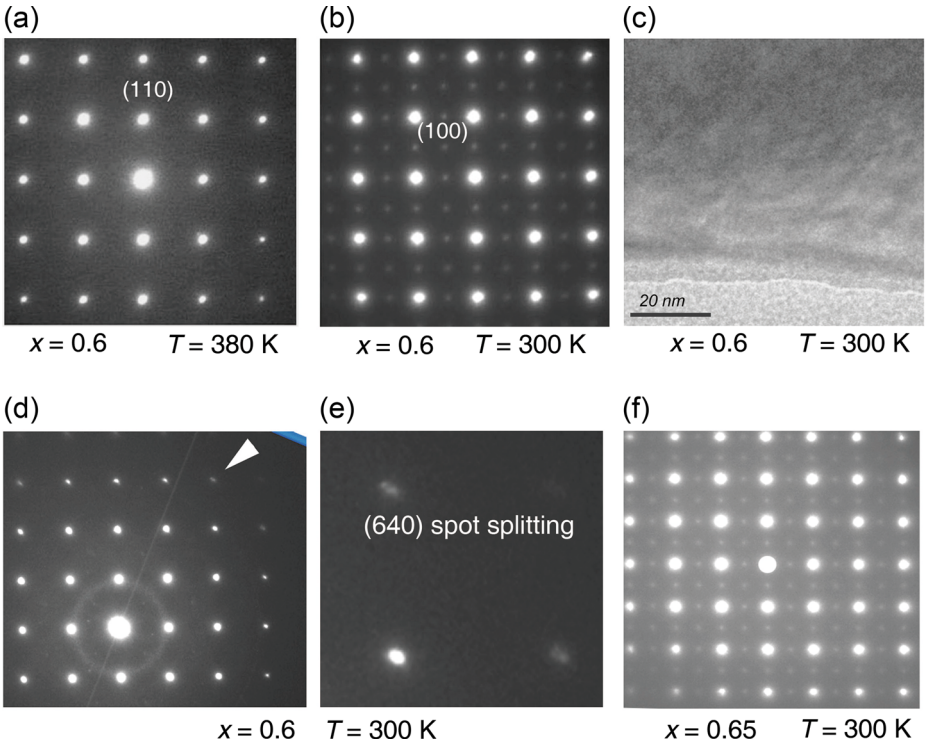

Fig. 7 Electron diffraction patterns of $LaFeAsO_{0.4}F_{0.6}$ and $LaFeAsO_{0.35}F_{0.65}$. **a b** TEM data for $x = 0.6$ at $T = 380$ K and 300 K. The images were taken along the [001] zone-axis direction. **c** The domain structures for $x = 0.6$ at $T = 300$ K **d** The splitting of some diffraction spots for $x = 0.6$ at $T = 300$ K. The images were rotated by 4 degrees in order to see the splitting more clearly. The (100) spots appear weak after such rotation. **e** A blow-up for the (640) diffraction spot indicated by the write arrow in (**d**). **f** The TEM image for $x = 0.65$ at $T = 300$ K

at $T = 300$ K for $x = 0.65$, which indicates that the $C4$ symmetry is also broken already at room temperature for this composition. The TEM results are in agreement with the NMR data of $T_s > 300$ K for $x \geq 0.6$.

Recently, the electronic nematicity (in-plane anisotropy) has been a main focus in the study of iron-pnictides. In LaFeAsO or underdoped $BaFe_{2-x}M_xAs_2$ (M = Ni, Co), a structural transition takes place above the magnetic order temperature T_N [13–15]. Below or even above T_s, many physical properties exhibit strong anisotropy [11, 16, 17]. It has been proposed that the structural transition, the electronic nematicity, the magnetic transition and the superconductivity are inter-related [18]. Currently, there are two schools of theories. One is that the structural transition and the resulting electronic nematicity are of spin origin [19]. However, the situation is completely different in the present case. Our system is far away from a magnetic ordered phase, and there is no indication of low-energy magnetic fluctuations. Figure 8 shows the temperature dependence of $1/T_1T$ and K for high-doping $0.3 \leq x \leq 0.75$ samples. The two quantities both decrease with decreasing temperature, suggesting that they are dominated by the density of states at the Fermi level as in weakly-correlated metals. This is in sharp contrast to the low-doping region ($x \leq 0.15$) where $1/T_1T$ increases rapidly upon cooling [6], due to the significant low-energy antiferromagnetic spin

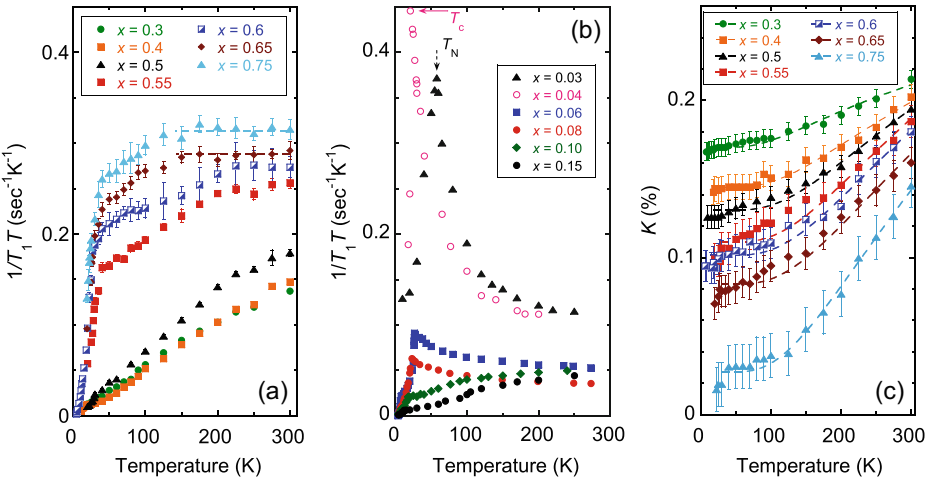

Fig. 8 The quantity $1/T_1T$ and the Knight shift. **a** The variation of $1/T_1T$ for $x \geq 0.3$. The broken lines show a $1/T_1T$ = const. relation. **b** Data for $x \leq 0.15$ taken from Ref. [6]. **c** The temperature dependence of the Knight shift K of $H_0 \parallel ab$ for $x \geq 0.3$

fluctuations. One possibility is that the spin fluctuations are transferred to high energy in the high-doping regime of our system. It is a future task to elucidate how such fluctuations are related to superconductivity.

The second school of theories is that orbital order or fluctuations are responsible for the nematic structural transition and the superconductivity. However, such orbital fluctuations can be enhanced only when spin fluctuations exist [20, 21]. Thus, in the present case where low-energy magnetic fluctuations are absent, the observed T-linear resistivity will lead to some new clues. The T-linear behavior of resistivity seen around $x_{\rm opt}$ may be caused by the fluctuations of widely-searched orbital order. In fact, a similar T-linear resistivity was found in $BaFe_{2-x}Ni_xAs_2$ (x=0.14) which is far away from the magnetic quantum critical point (x=0.10) and T_s extrapolates to zero there [15].

Finally, we discuss the properties of the superconducting state. Figure 9a shows the temperature dependence of the spin-lattice relaxation rate $1/T_1$ for the new dome. For all F-concentrations, there is a clear and sharp decrease below T_c. Figure 9b shows the temperature dependence of $1/T_1$ for x=0.6, in comparison with that for x=0.08 in the first dome. As for x=0.08 reported earlier [22], $1/T_1$ decreases rapidly without a Hebel-Slichter (coherence) peak and a hump was seen around T= 9 K, which is an indication of multiple gaps [6]. The same feature was seen in the optimally-doped $Ba_{1-x}K_xFe_2As_2$ [23]. The similar temperature dependence and hump structure are also seen in the x = 0.6 compound, suggesting the identical gap symmetry. For the semi-log plot of $1/T_1$ *vs* T_c/T as shown in the inset, both compounds fall on two different straight lines. Since a straight line in such a semi-log plot means that $1/T_1$ follows an $exp(-\Delta/T)$ relation (Δ is a constant), multiple fully-opened gaps seem to be realized under the new dome as well.

our work suggests that, the heavily F-doped $LaFeAsO_{1-x}F_x$ system made by the high-pressure synthesis technique represents a unprecedented class of superconductors, and provides new chance to study the electronic nematicity and related quantum criticality. In addition to the conventional phonon or magnetic fluctuations mechanisms, there may be a new route to high temperature superconductivity. Moreover, we emphasize that the phase

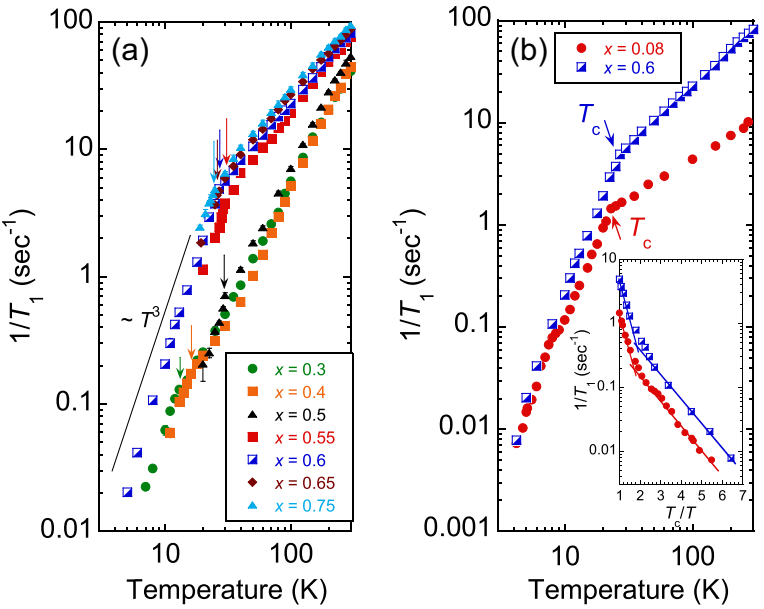

Fig. 9 **a** The temperature dependence of the ^{75}As spin-lattice relaxation rate $1/T_1$. The arrows indicate T_c under the magnetic field of $H \sim 12$ T measured by the $in-situ$ NMR coil. The straight line is a guide to the eyes to indicate the $1/T_1 \propto T^3$ relation. **b** Comparison of the nuclear spin-lattice relaxation rate in the superconducting state for x=0.08 and 0.6. The inset shows the $1/T_1$ below T_c as a function T_c/T in a semi-log plot for the two compounds. A straight line in such a plot means that $1/T_1$ follows an $exp(-\Delta/T)$ relation

diagram discovered here resembles that of heavy fermion compound $CeCu_2Si_2$ where two superconducting phases were reported [24]. Our work may also sheds light on the physics of heavy fermion materials such as $CeCu_2Si_2$.

4 Conclusion

In summary, we have reported the discovery of a new superconductivity dome in $LaFeAsO_{1-x}F_x$ with $0.25 \leq x \leq 0.75$ synthesized by using the high-pressure technique, where the maximal critical temperature T_c at $x_{opt} = 0.5 \sim 0.55$ is even higher than that at $x \leq 0.2$. Over the entire new dome, there is no indication of low-energy magnetic fluctuations as evidenced by the temperature dependence of the spin-lattice relaxation rate $1/T_1T$. Instead, by nuclear magnetic resonance and transmission electron microscopy, we find a new type of phase transition takes place above the dome, below which the $C4$ rotation symmetry is broken. The electrical resistivity is linear in temperature around the doping level where the crystal transition temperature extrapolate to zero and T_c is the maximal, which suggests the importance of quantum fluctuations associated with the structural transition. Our results point to a new paradigm of high temperature superconductivity, and suggest that there may be a new route to high temperature superconductivity and that superconductors with further higher T_c await discovery.

Acknowledgements This work was done in collaboration with R. Zhou, Z. Z. Zhao, J. Q. Li, H. X. Yang and L. L. Wei of Institute of Physics, CAS. This work was supported by CAS's Strategic Priority Research Program, No. XDB07020200, National Basic Research Program of China, Nos. 2012CB821402, 2011CBA00109 and by NSFC Grant No 11204362.

References

1. Kamihara, Y., Watanabe, T., Hirano, M., Hosono, H.: J. Am. Chem. Soc **130**, 3296 (2008)
2. Ren, Z.A., Lu, W., Yang, J., Yi, W., Shen, X.L., Li, Z.C., Che, G.C., Dong, X.L., Sun, L.L., Zhou, F., Zhao, Z.X.: Chin. Phys. Lett. **25**, 2215 (2008)
3. Lee, P.A., Nagaosa, N., Wen, X.G.: Rev. Mod. Phys. **78**, 17 (2006)
4. Mathur, N.D., Grosche, F.M., Julian, S.R., Walker, I.R., Freye, D.M., Haselwimmer, R.K.W., Lonzarich, G.G.: Magnetically mediated superconductivity in heavy fermion compounds. Nature **394**, 39 (1998)
5. Luetkens, H., Klauss, H.H., Kraken, M., Litterst, F.J., Dellmann, T., Klingeler, R., Hess, C., Khasanov, R., Amato, A., Baines, C., Kosmala, M., Schumann, O.J., Braden, M., Hamann-Borrero, J., Leps, N., Kondrat, A., Behr, G., Werner, J., Buechner, B.: Nat. Mater. **8**, 305 (2009)
6. Oka, T., Li, Z., Kawasaki, S., Chen, G.F., Wang, N.L., Zheng, G.-Q.: Phys. Rev. Lett. **108**, 047001 (2012)
7. Yang, J., Zhou, R., Wei, L.L., Yang, H.X., Li, J.Q., Zhao, Z.X., Zheng, G.-Q.: Chin. Phys. Lett. **32**, 107401 (2015)
8. Narath, A.: Phys. Rev. **162**, 320 (1967)
9. Matano, K., Ren, Z.A., Dong, X.L., Sun, L.L., Zhao, Z.X., Zheng, G.-Q.: Europhys. Lett. **83**, 57001 (2008)
10. Abragam, A.: *The Principles of Nuclear Magnetism*. Oxford University Press, London (1961)
11. Fu, M., Torchetti, D.A., Imai, T., Ning, F.L., Yan, J.Q., Sefat, A.S.: Phys. Rev. Lett. **109**, 247001 (2012)
12. Ma, C., Zeng, L.J., Yang, H.X., Shi, H.L., Che, R.C., Liang, C.Y., Qin, Y.B., Chen, G.F., Ren, Z.A., Li, J.Q.: Europhys. Lett. **84**, 47002 (2008)
13. de la Cruz, C., Huang, Q., Lynn, J.W., Li, J.Y., Ratcliff, W.I.I., Zarestky, J.L., Mook, H.A., Chen, G.F., Luo, J.L., Wang, N.L., Dai, P.C.: Nature **453**, 899 (2008)
14. Sefat, A.S., Jin, R., McGuire, M.A., Sales, B.C., Singh, D.J., Mandrus, D.: Phys. Rev. Lett. **101**, 117004 (2008)
15. Zhou, R., Li, Z., Yang, J., Sun, D.L., Lin, C.T., Zheng G.-Q.: Nat. Commun. **4**, 2265 (2013)
16. Chu, J.H., Analytis, J.G., De Greve, K., McMahon, P.L., Islam, Z., Yamamoto, Y., Fisher, I.R.: Science **329**, 824 (2010)
17. Yi, M., Lu, D.H., Chu, J.H., Analytis, J.G., Sorinia, A.P., Kemper, A.F., Moritz, B., Mod, S.K., Moore, R.G., Hashimoto, M., Lee, W.S., Hussain, Z., Devereaux, T.P., Fisher, I.R., Shen, Z.X.: Natl. Acad. Sci. USA **108**, 6878 (2011)
18. Fernandes, R.M., Chubukov, A.V., Schmalian, J.: Nat. Phys. **10**, 97 (2014)
19. Fernandes, R.M., Bohmer, A.E., Meingast, C., Schmalian, J.: Phys. Rev. Lett. **111**, 137001 (2013)
20. Kontani, H., Onari, S.: Phys. Rev. Lett. **104**, 157001 (2010)
21. Lee, C.C., Yin, W.G., Ku, W.: Phys. Rev. Lett **103**, 267001 (2009)
22. Kawasaki, S., Shimada, K., Chen, G.F., Luo, J.L., Wang, N.L., Zheng G.-Q.: Phys. Rev. B **78**(R), 220506 (2008)
23. Li, Z., et al.: Phys. Rev. B **83**(R), 140506 (2011)
24. Yuan, H.Q., Grosche, F.M., Deppe, M., Geibel, C., Sparn, G., Steglich, F. Science **302**, 2104 (2003)